geosciences

MDPI

Article

Petrographic and Petrophysical Characterization of Detrital Reservoir Rocks for CO_2 Geological Storage (Utrillas and Escucha Sandstones, Northern Spain)

Félix Mateos-Redondo [1], Timea Kovács [2] and Edgar Berrezueta [3,*]

[1] Gea Asesoría Geológica, Polígono de Silvota, C/Peña Beza, Nave 16, 33192 Llanera, Spain; felix@geaasesoriageologica.com
[2] Freelance consultant, C/La Estrecha, 46, 16Q 4° Izq, 33011 Oviedo, Spain; kovacstim@gmail.com
[3] Instituto Geológico y Minero de España (IGME), C/Matemático Pedrayes 25, 33005 Oviedo, Spain
* Correspondence: e.berrezueta@igme.es; Tel.: +34-609-381-623

Received: 4 June 2018; Accepted: 29 June 2018; Published: 3 July 2018

Abstract: The aim of this article is to provide a qualitative and quantitative description of Lower–Upper Cretaceous detrital rocks (Escucha and Utrillas sandstones) in order to explore their potential use as CO_2 reservoirs based on their petrographic and petrophysical characteristics. Optical microscopy (OpM) and scanning electron microscopy (SEM) aided by optical image analysis (OIA) were used to get qualitative and quantitative information about mineralogy, texture and pore network structure. Complementary analyses by X-ray fluorescence (XRF) and X-ray diffraction (XRD) were performed to refine the mineralogical information and to obtain whole rock geochemical data. Furthermore, mercury injection capillary pressure analysis (MICP), the gas permeameter test (GPT) and the hydraulic test (HT) were applied to assess the potential storage capacity and the facility of fluid flow through the rocks. Both of these factors have an outstanding importance in the determination of CO_2 reservoir potential. The applied petrophysical and petrographic methods allowed an exhaustive characterization of the samples and a preliminary assessment of their potential as a CO_2 reservoir. The studied conglomerates and sandstones have a porosity range of 8–26% with a dominant pore size range of 80–500 μm. The grain skeleton consists of quartz (95%), very minor potassium feldspars (orthoclase) and a small amount of mica (muscovite and chlorite). According to these preliminary results, among the studied varieties, the Escucha sandstones have the most favorable properties for CO_2 geological storage at the rock matrix scale.

Keywords: petrographic; petrophysical; detrital reservoir; CO_2 geological storage

1. Introduction and Objectives

Carbon Capture and Storage (CCS) is one possible option for reducing greenhouse gas concentration in the atmosphere. The last step of the process is the geological CO_2 storage, during which the compressed gas is injected into a porous rock formation for its permanent disposal [1,2]. Adequate geological environments for CO_2 storage are provided by depleted hydrocarbon reservoirs, deep coal seams and saline aquifers. In Spain, deep saline aquifers have the highest potential to be used in industrial scale CCS projects [3].

These geological structures consist of porous and permeable sedimentary rocks containing a fluid of high salinity (brine) in the voids that exist among the rock forming grains (in sandstones) or in fissures and dissolution cavities (in carbonates). They usually are confined due to their structural position and are deeper than fresh water aquifers. Conceptually, CO_2 storage in saline aquifers aims to reproduce the conditions of natural hydrocarbon reservoirs [2–6].

Any site selected for geological storage must comply with a series of requirements guaranteeing safe operation and permanent confinement, such as >800 m depth, geologically stable area, and sufficient storage capacity, among others.

Intrinsic petrophysical and geochemical properties of the reservoir and seal rock formations are key to the feasibility of CO_2 geological storage projects [4].

By the combination of a series of routine and advanced laboratory techniques, these properties can be effectively and meaningfully determined both qualitatively and quantitatively. The results of rock characterization provide valuable information for modelling and assessing fundamental reservoir properties, such as injectivity, storage capacity or reactive processes [4,7–11]. As far as injectivity is concerned, the porosity and permeability of the reservoir rock and the chemical reactions in the CO_2-brine-rock system (i.e., mineral dissolution/precipitation) are decisive [4,12].

Ideally, a set of full core samples produced from wells at or near the proposed storage site are used for reservoir characterization studies [13,14]. The accessibility of this kind of samples, however, is often limited or is only secured at advanced stages of the project. In areas like Spain, due to the lack of significant hydrocarbon resources, deep geological data of any kind is rather scarce. In these cases, outcrop analogues could be used to obtain preliminary information about target geological formations. Keeping in mind the possible alterations suffered by the materials that has reached surface exposure, the study of outcrop samples can provide a simple and fast way to determine the potentiality of a given geological formation for its use as a CO_2 reservoir.

This study is aimed at (i) describing the petrographic and petrophysical characterization of detrital sedimentary rocks with potential to be used as CO_2 reservoir; (ii) discussing the suitability of the selected rocks for CO_2 storage based on the obtained results; (iii) assessing the value of data measured on outcrop samples through a case study (Utrillas and Escucha Sandstones).

Therefore, this paper provides an overview of the process and results of a preliminary characterization methodology that can serve as a basis for more detailed and specific studies of CO_2 reservoir rocks. The overall, representative characterization of surface outcrops, which remains out of the scope of this study, would require a larger number of samples than the one used here. Our main focus was to provide data for verification of the methodology.

The Utrillas and Escucha sandstones were selected for this study due to their importance as potential CO_2 reservoir rocks. Their lithological characteristics and structural position make them possible candidates for Spanish CO_2 geological storage projects [3,15]. Potential reservoir structures have been identified in the Duero basin (Figure 1a) that comply with the requirements for CO_2 geological storage, in which the reservoir is composed of these sandstones [16]. The sandstones were sampled for this study in two different zones, north of the Duero Basin, where they outcrop on the surface (Figure 1b,c). The corresponding caprock formations do not appear in the studied surface outcrops.

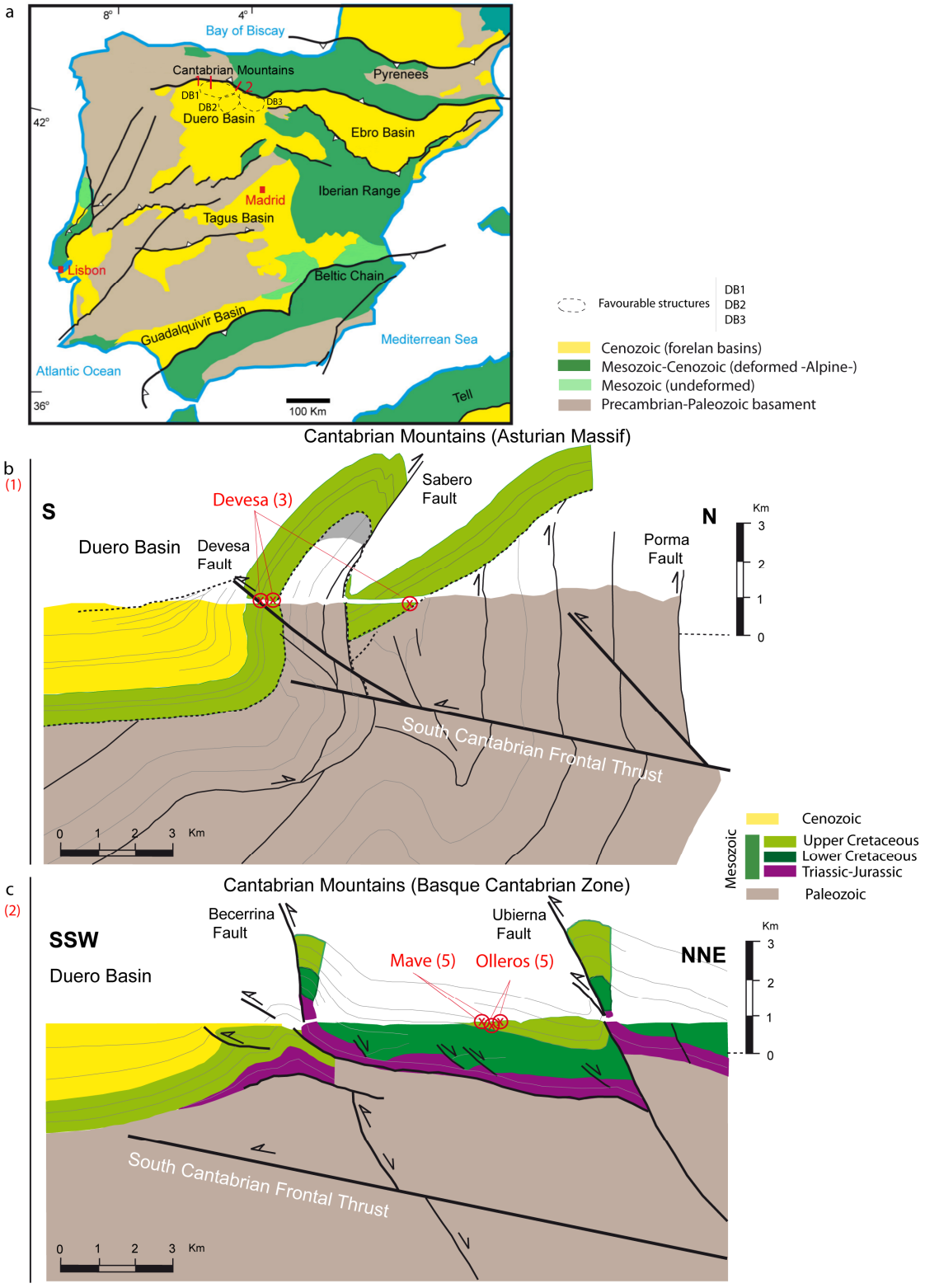

Figure 1. (**a**) Location of study areas with basic geological information: sampling areas Devesa (1) and Olleros-Mave (2) and favorable structures for CO_2 storage [16]; (**b**) Geological cross-section along the Devesa study area showing the positions of the sampling sites (Devesa 1 to 3); (**c**) Geological cross-section along the Olleros-Mave study area showing the positions of the sampling sites (Olleros 1 to 5 and Mave 1 to 5). Modified from [7].

2. Geological Setting

According to [16], in the north of Spain, the Duero Basin (Figure 1a) is considered the principal potential CO_2 storage zone. In detail, three favorable structures have been identified at the northern border of the Duero basin (Figure 1a): Duero Basin 1 (DB-1) (antiform cut by faults in thrust structure), DB-2 (antiform in thrust structure) and DB-3 (anticline sealed by reverse faults). In these three structures, the reservoir rocks could be either Escucha sandstones (Aptian–Lower Albian age) or Utrillas sandstones (Upper Albian–Lower Cenomanian age). Clays and marls of Cenomanian age provide a suitable cap-rock [16].

The target reservoir formations of the present study belong to Cretaceous materials situated between the Cantabrian Mountains and the Duero Basin (Figure 1a). The older Escucha sandstones are dated to the Aptian–Lower Albian age, while the younger unit, which is commonly known as Utrillas sandstones, is dated to the Upper Albian–Lower Cenomanian age. They are mainly composed of loose conglomerates and whitish sandstones deposited in a continental-fluvial environment. The Escucha and Utrillas sandstones were formed in an extensional setting that affected Northern Spain and produced the opening of the Bay of Biscay [17]. The Escucha sandstones were deposited during the tectonic subsidence phase and Utrillas sandstones during the thermal subsidence episode.

These units were sampled in two different zones. The first one (Figure 1a) is situated in the vicinity of the village of Boñar and is referred to as "Devesa zone" in this work, after Devesa de Boñar. The second zone (Figure 1a) was selected close to the village of Olleros de Pisuerga and was named "Olleros-Mave zone". Although both Devesa and Olleros are located at the transition zone between the Cantabrian Mountains and the Duero Basin and have similar structural positions, there are some stratigraphic differences between them.

In the first study area (Figure 1b) only the Utrillas sandstones crop out. This formation belongs to a Cretaceous sequence that lays unconformably on the Paleozoic basement of the Variscan Cantabrian Zone (Asturian massif). On top of the Cretaceous sequence, a succession of almost 2500 m thick Cenozoic materials was deposited in the Duero Basin. The Utrillas sandstones have a thickness of approx. 250 m and are composed of conglomerates at the base with a progressively increasing sandstone ratio. These sandstones were formed in a fluvial braided environment with a source area composed of acid, mainly granitic and metamorphic rocks [18]. The structure of the sampling area is characterized by a complex monocline (Figure 1b) that has been related with a south-directed basement thrust inclined to the north [19].

The second study area is situated at the SW border of the Basque-Cantabrian Zone (Figure 1c), which is principally comprised of sedimentary sequences from the Triassic to the Tertiary age [20]. Here both the Escucha and the Utrillas sandstones outcrop on the surface. The Escucha sandstones show variable thicknesses of 200–500 m. They are composed of conglomeratic and sandy facies formed in fluvial environments [18]. The outcrops of the Utrillas sandstones reveal thicknesses of 100–500 m. They usually appear in small anticline structures. The current structure of this border between the Cantabrian Mountains and the Duero basin has been related also with a basement thrust dipping to the north [21]. A geological cross section in Figure 1c illustrates the structural characteristics of the area.

In general, the Escucha sandstones are composed of fluvio-alluvial facies of braided type that present a great lateral and vertical variety as far as type and proportion of channel and intercanal deposits are concerned [18]. The Utrillas sandstones are composed of detrital, poorly consolidated or unconsolidated whitish materials ranging from sandstone to conglomerate, with a maximum size of pebbles of 6 cm [22,23]. The fluvial environment, in which the Utrillas sandstones were formed, represents the proximal part of the upper Cretaceous north Iberian palaeomargin. The Utrillas sandstones were sampled at three sites in the Devesa area (Devesa 1 to 3) and at five sites in the Olleros-Mave area (Olleros 1 to 5). The Escucha sandstones were sampled at five sites in the Olleros-Mave area (Mave 1 to 5).

3. Methodology

The overall methodology to study the petrographic and petrophysical characterization of detrital rocks consisted of the following steps (Figure 2a):

- Selection of a study area with real potential for CO_2 geological storage.
- Locating surface outcrops of the target reservoir rocks and sampling.
- Sample preparation for laboratory studies.
- Petrographic and geochemical characterization of samples.
- Petrophysical characterization of samples.
- Interpretation of results and correlation of petrographic and petrophysical data.

Applied Techniques and Methods

This study addresses the petrographic and petrophysical characterization of rocks with potential to be used as CO_2 reservoirs. A study area was selected in Spain that, according to previous research, meets the requirements for CO_2 geological storage. After the site selection, the potential reservoir rock formations were identified and sampled. All the samples were taken from surface outcrops by means of shallow (1 m) boreholes (Figure 2b). Samples afterwards were dried and prepared for their characterization.

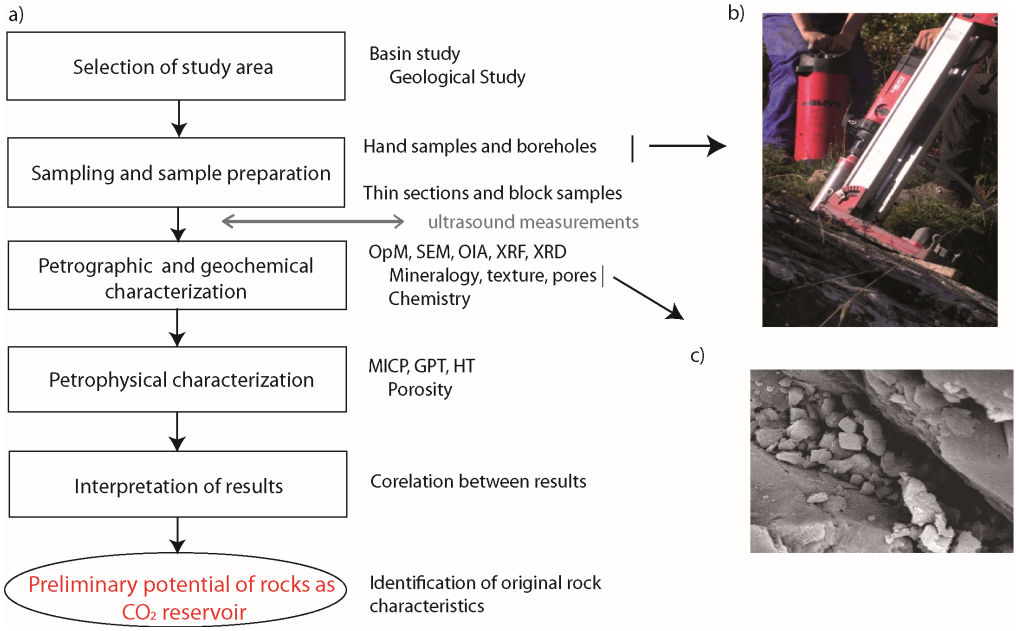

Figure 2. (**a**) Schematic representation of the work sequence followed in this study; (**b**) sampling; (**c**) SEM image of the studied sandstones.

The first properties to assess were the rock heterogeneity and anisotropy, as they condition the sampling and sample preparation strategies concerning the number, size, location and orientation of samples. Due to their relevance, these two properties were studied in detail both "in situ" and in the laboratory [24], applying a non-destructive technique (NDT) based on the propagation of ultrasound waves. The direct transmission of P and S waves (Pundit Plus-CNS-Farnell with 1MHz transducers) provides information about the petrographic components with special emphasis on the porosity, micro-fissures, density and alteration degree and their orientation. Afterwards, samples were prepared for further laboratory studies and experimentation (cores, plugs, thin sections, etc.).

The first step of the petrographic characterization was the observation of thin sections by means of optical microscopy (OpM) using a Leica DM 6000 polarization microscope (magnification of 10×),

which provided qualitative information about the mineralogical composition, texture and porosity of the samples. By the application of optical image analysis (OIA by ImageJ software) on images acquired from thin sections, it was possible to quantitatively assess pore space parameters, such as porosity (A %), mean pore diameter and pore shape. The segmentation of the porous system on OpM and SEM images were made by regions, applying the "thresholding" segmentation method (based on threshold values to turn a raw image into a binary one, the pixels being partitioned according to their intensity value). Pore clusters were measured in this step. The pore clusters were defined as continuous pore spaces that are not in contact with each other and they may consist of various individual pores.

The petrographic characterization was further completed by X-ray fluorescence chemical analysis (XRF) using a PHILIPS PW2404 spectrometer and X-ray diffraction mineralogical analysis (XRD) using a PHILIPS X´PERT PRO diffractometer. The PANalytical X'Pert HighScore Plus software and the PDF4 data base were applied for phase identification and the XPowder software and RRUFF data base for quantification. For XRF and XRD analyses, whole rock samples were crushed manually in an agate mortar to 1µm grain size. Furthermore, Scanning Electron Microscopy with back-scattered electrons (SEM-BSE, JEOL 6100 SEM, using W-Filament, acceleration voltage of 20 kV and Inca Energy-200 software) was used for detailed observation of mineralogical and pore space properties (Figure 2c).

The petrophysical characterization, at rock matrix scale, included the assessment of hydraulic properties, pore space configuration and hydraulic functionality of the samples. Using representative sample volumes (i.e., cm-dm scaled cores) and an automatized measurement method (AUTOSORC) [25], we studied how much water the rocks take up, how easily the liquid moves through the rock matrix and the kinetics of this movement, which allowed us to determine parameters, such as porosity (effective, not effective and closed), capillary uptake, permeability, water absorption and desorption [26–30]. Samples used for AUTOSORC measurements were 10 cm in diameter and 20–25 cm in length. Small cores of 3.72 cm in diameter and 2.54–7.62 cm in length were used for permeability measurements, applying 2.41 MPa of confining pressure and 0.006 to 0.68 MPa starting pressures. Measurements were also carried out on powdered samples using a Le Chatelier pycnometer to refine some of the petrophysical parameters.

Furthermore, by means of mercury intrusion porosimetry (MCIP-Micromeritics AUTOPORE IV with 33,000 psi maximum pressure and 360–0.0001 µm detectable pore throat radius range) the volume, geometry and distribution of voids (i.e., pore space configuration) of smaller plugs (2.1 cm in diameter and 2.6 cm in length) were assessed. This method highlights the properties of the channels that connect the pores, or pore throats, including the distribution of their radii and their tortuosity. These factors are decisive in the degree of connectivity of the pore space, and therefore, in the ease with which fluids will circulate through the porous medium. By the combined interpretation of the hydraulic properties and the pore space configuration, we can assess the rock hydraulic functionality at the rock matrix scale. For this purpose, the above parameters, and especially the intrusion and extrusion curves of MCIP, were used as an input in a 3D simulation of fluid circulation by means of the Pore-Cor RS 6.0 suite [8,25,31,32].

4. Results

4.1. Heterogeneity and Anisotropy

Mean P-wave velocity (Vp) values were found to be 1332 ± 236 m/s for the Escucha sandstones and 3073 ± 478 m/s for the Utrillas sandstones. This notable difference in Vp sheds light on the differences in the porosity of the two formations, being the porosity of Escucha significantly higher. Velocity values also tend to be lower in the direction of the Z-Z' axis (i.e., vertically) than in the horizontal directions in both formations (see an example in Figure 3). The Vp drop is about 32% in the Utrillas sandstones (Olleros zone) and 8% in the Escucha sandstones. This reflects a certain degree of anisotropy, which is higher in the first case (mean coefficient of anisotropy = 1.4) than in the second one (mean coefficient of anisotropy = 1.1). On the other hand, the calculated residual times reveal the

heterogeneous nature of the materials on the studied cm-dm scale [5,25]. The heterogeneity detected along the cores suggests the existence of layers of higher and lower porosity (Figure 3).

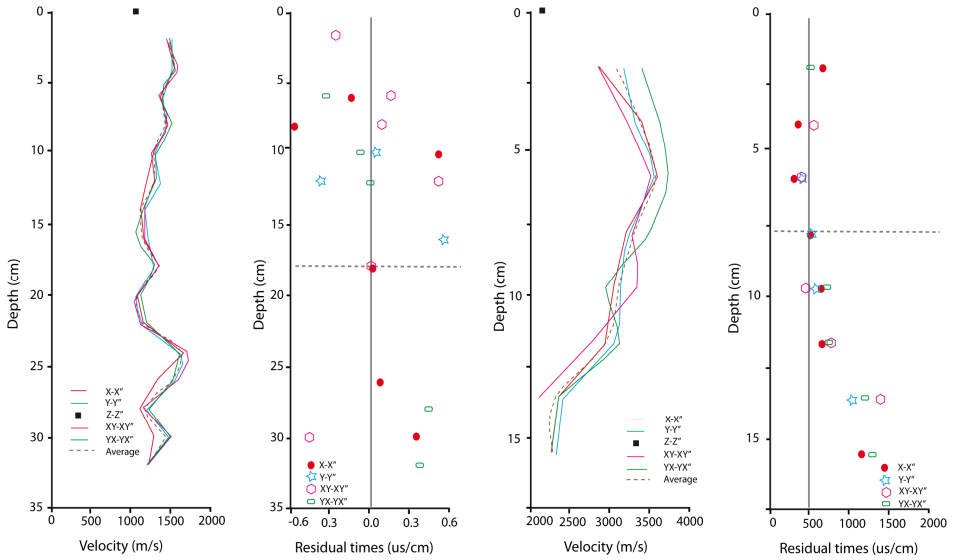

Figure 3. Examples of the results of ultrasound measurements (P-wave velocity and residual time values) on one sample of the Escucha sandstones (Mave site) (**left**) and one of the Utrillas sandstones (Olleros site) (**right**). Both the vertical/horizontal anisotropy and the heterogeneity are more significant in the Utrillas sansdstones.

4.2. Petrographic and Chemical Characterization

The Utrillas and Escucha sandstones are mainly composed of loose conglomerates and whitish sandstones deposited in a continental-fluvial environment. The principal difference between the varieties lays in the grain size distribution and the degree of consolidation. Four thin sections were studied for each variety of the Utrillas sandstones and five thin sections for the Escucha sandstones.

The sampled Escucha sandstones are well sorted, grain supported quartz arenites (Figures 4a and 5a). Mono- and polycrystalline quartz grains are subrounded to rounded with medium sphericity and commonly form about 95 percent of the sand. A small amount of potassium feldspars are also present, usually showing signs of alteration with Fe-oxide and mica/clay mineral replacements (Figure 4b). The average grain size of these components is 150–250 μm. A detrital matrix (<5%) formed by quartz, feldspar, clay (kaolinite, illite, smectite) and mica (muscovite) grains bind the framework together with scarce presence of Fe-oxides. An average porosity of about 15% is made up by intergranular porosity and intracrsystalline fissures in the quartz grains. No textural or mineral orientation can be observed.

The Utrillas sandstones are heterogeneous, medium to coarse grained quartz arenites, occasionally classified as conglomeratic sandstone. Over 90–95% of the grains are mono- and polycrystalline quartz of highly variable grain size from 100 μm to >2000 μm, which rends the rock a poorly sorted, heterogeneous texture (Figures 4c and 5b). Grain shapes also vary from subangular to rounded. Smaller amount of feldspars, mica (muscovite), clay minerals (illite, chlorite, kaolinite) were observed. The amount of matrix is usually lower than 5% but in some zones it may go up to 15%. It is mainly composed of quartz, phyllosilicates and opaque minerals. The presence of Fe-oxides and hydroxides (hematite and limonite) in the matrix is more dominant in the Olleros samples (Figures 4d and 5c). The average porosity is about 10% with secondary intercrystalline voids and a significant degree of microfracturation in the quartz grains sometimes filled with Fe-oxides.

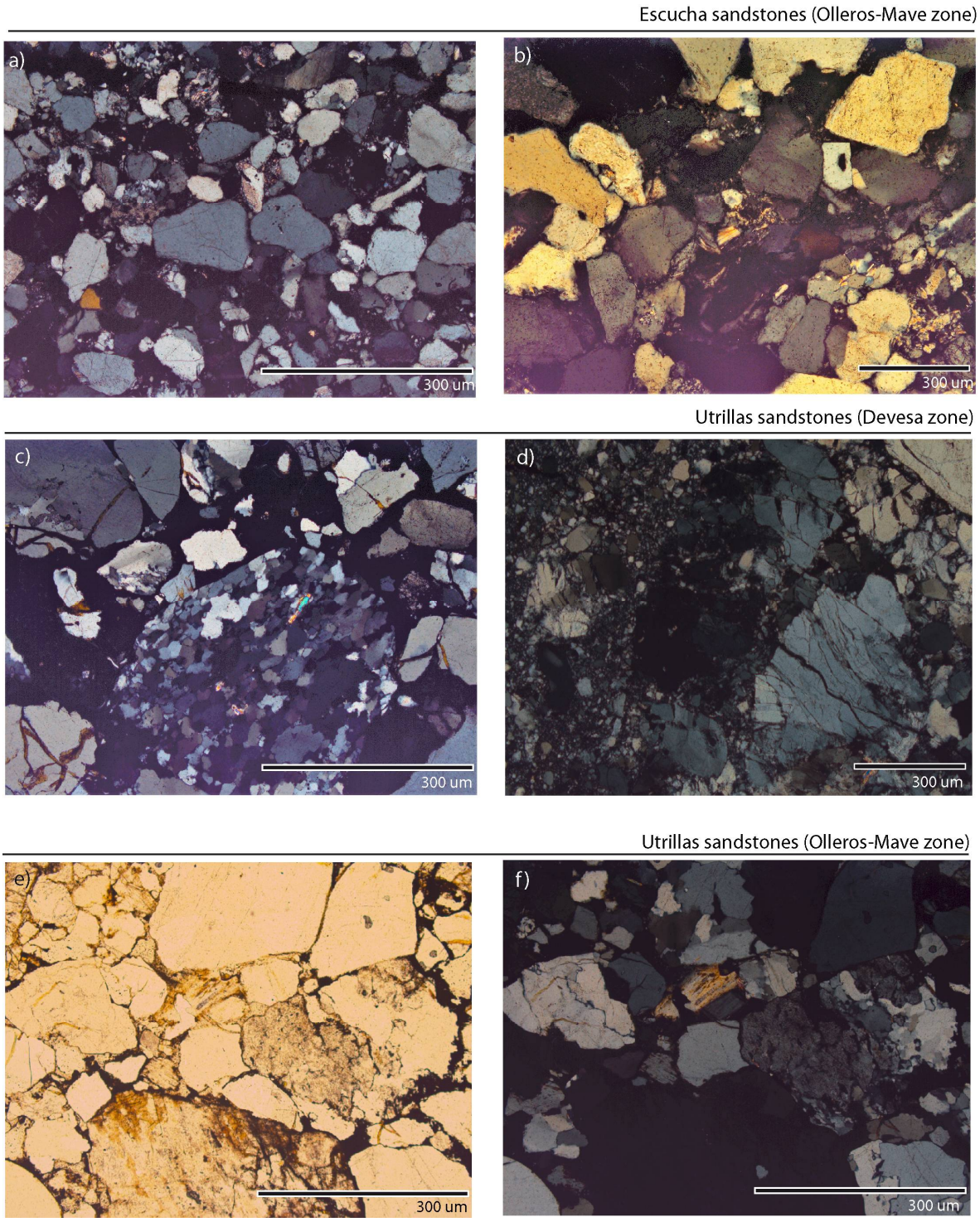

Figure 4. Characteristic textural features of the detrital rocks observed by OpM. (**a**) Homogeneous grain size and dominantly quartz composition of the Escucha sandstones (Mave site) with a tourmaline crystal. Crossed nicols, 5×. (**b**) Quartz, feldspar and phyllosilicate components in the Escucha sandstones (Mave site). Crossed nicols, 10×. (**c**) Mono- and polycrystalline quarts grains of highly heterogeneous size in the Utrillas sandstones (Devesa site). Crossed nicols, 5×. (**d**) Quartz in the Utrillas sandstones (Devesa site). Crossed nicols, 5×. (**e**,**f**) Significant Fe-oxide, -hydroxide content in the matrix of the Utrillas sandstone (Olleros site). Crossed and parallel nicols, 5×.

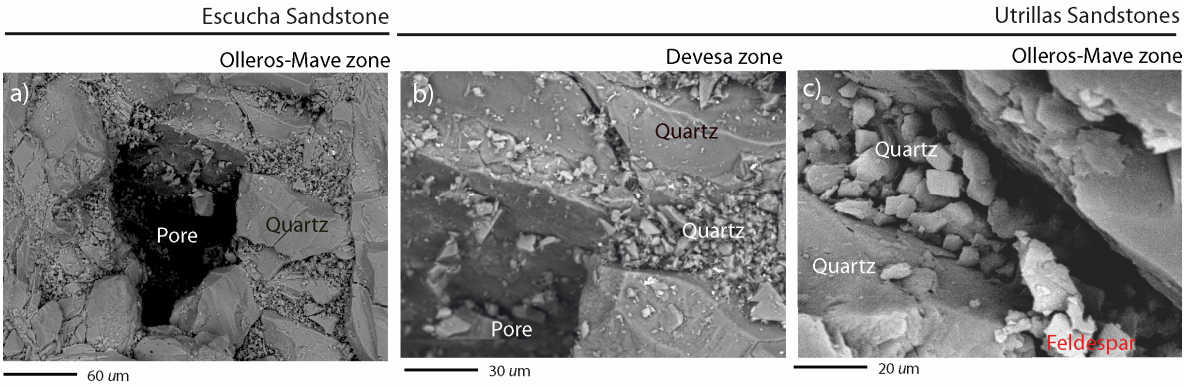

Figure 5. Characteristic textural features of the detrital rocks observed by SEM. (**a**) Homogeneous grain size and dominantly quartz composition of the Escucha sandstones (Mave site). (**b**,**c**) Mono- and polycrystalline quarts grains of highly heterogeneous size in the Utrillas sandstones (Devesa site and Olleros site).

A first pore network quantification by OIA-OpM and OIA-SEM was carried out on thin sections (8 of Utrillas and 5 of Escucha). OIA-OpM was applied on images acquired with a magnification of 10× and was mainly focused on the measurement of geometric parameters in 2 dimensions (2D), such as roundness (Ro) and aspect ratio (As) [33] (Table 1). Pore size is expressed as the mean ferret diameter measured as the best fitted ellipse to the pore [34]. The estimated porosity percentage ranges from 9.3 to 21.7% with an average of 17.35 for the Escucha sandstones (Mave site). The same parameter was found to be between 6.49 and 18.18% with an average of 14.65 for the Utrillas sandstone (Devesa site) and between 4.42 and 12.63% with an average of 7.78 for the Utrillas sandstone (Olleros site). The maximum and minimum pore area for the Utrillas samples is 172,100 and 9.2 μm^2, respectively, and the average pore area is 168 μm^2. In the case of Escucha sandstones, the maximum and minimum pore area is 240,200 and 9.2 μm^2, respectively, while the average is 241 μm^2.

Table 1. Optical porosity, roundness (Ro) and aspect ratio (As) measured by OIA-OPM of sandstones thin sections.

Samples		Porosity Average (%)	Ro Average	As Average
Escucha Sandstone Mave site		17.35	0.52	2.31
Utrillas sandstone	Devesa site	14.65	0.56	2.11
	Olleros site	7.78	0.55	2.14

OIA was also applied on SEM images (120 images of Escucha and 120 images of Utrillas sandstones) acquired with a magnification of 100×. Histograms of the obtained pore size distribution (expressed in radius) are shown in Figure 6. The dominant pore throat radii of the Escucha sandstones were found to be between 300–325 µm (14%) with a mean value of 275 µm. Pore throat radius values of the Utrillas sandstones are typically between 475–500 µm (12%) with a mean value of 250 µm. The pore size has bimodal distribution, in all the cases, with one peak between 0 and 250 µm and another one between 300 and 500 µm. The range of measurement was between 1 and 500 µm.

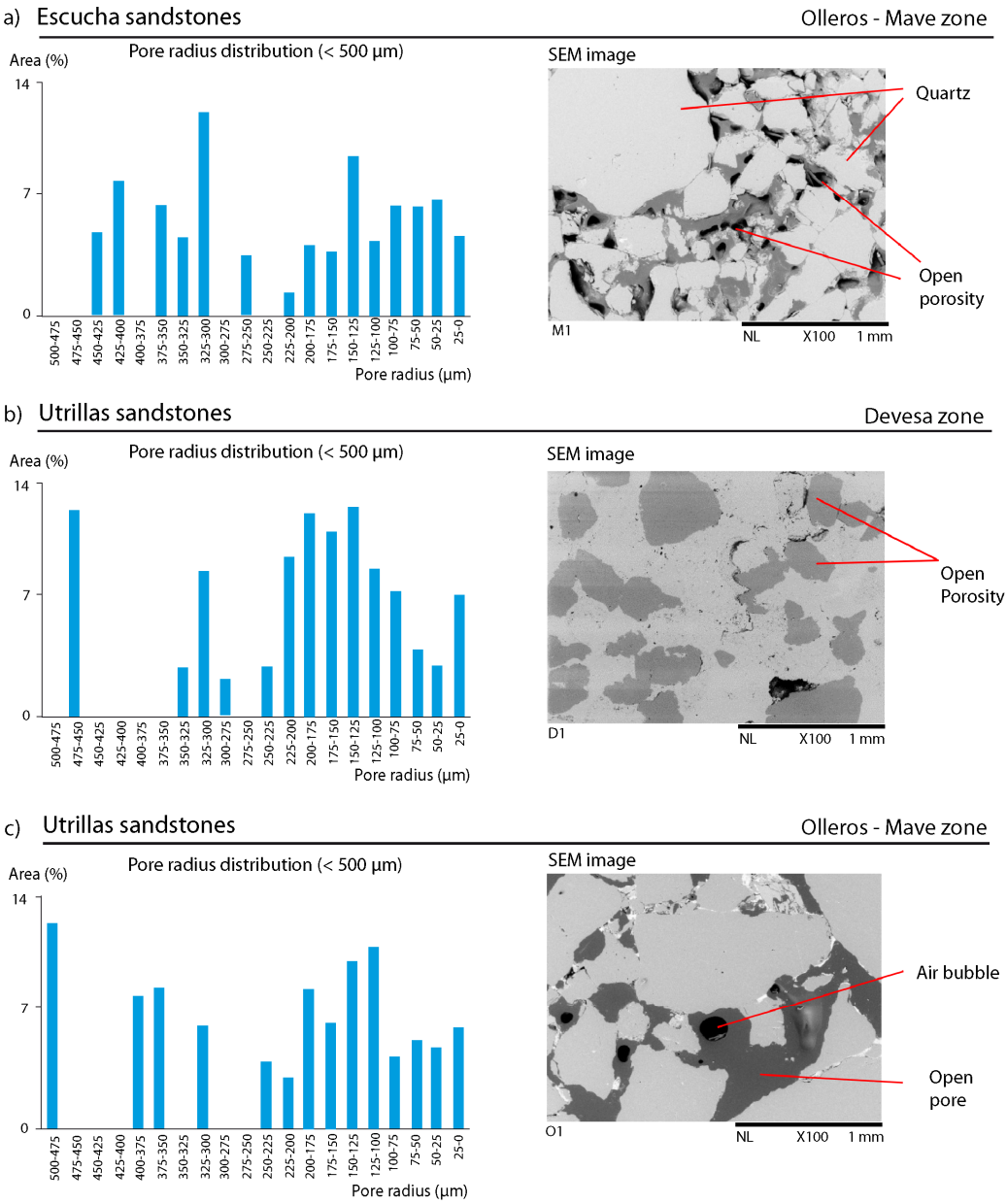

Figure 6. Pore size (radius) distribution histograms obtained by means of OIA-SEM (**a**) Escucha sandstones (Mave site); (**b**) Utrillas sandstones (Devesa site); (**c**) Utrillas sandstones (Olleros site). SEM images were obtained on samples impregnated with an epoxy resin in order to differentiate between open pores (dark grey) and minerals (light grey). Both closed pores and air bubbles resulting from imperfect impregnation appear in black color, which was taken into account and manually corrected during the digital image processing.

The whole rock chemical (XRF) and mineralogical (XRD) analyses confirmed the predominant quartz composition and the minor presence of aluminosilicates and Fe-minerals (Tables 2 and 3), in agreement with the OpM observations.

Table 2. Whole rock chemical composition. Mean values were calculated on the basis of 5 samples for each sandstone type.

Sample	SiO_2 (%)	Al_2O_3 (%)	Fe_2O_3 (%)	MnO (%)	MgO (%)	CaO (%)	Na_2O (%)	K_2O (%)	TiO_2 (%)	P_2O_5 (%)	L.O.I. (%)	TOTAL (%)
Escucha sandstone Mave site	95.64	1.39	0.58	0.00	0.04	0.01	0.03	0.13	0.32	0.02	0.92	99.08
Utrillas sandstone Devesa site	97.15	0.98	0.30	0.00	0.03	0.04	0.05	0.08	0.03	0.01	0.48	99.16
Utrillas sandstone Olleros site	96.95	0.90	0.32	0.00	0.02	0.04	0.05	0.08	0.03	0.01	0.52	98.92

Table 3. XRD mineralogical composition. Mean values were calculated on the basis of 5 samples for each sandstone type.

Sample	Quartz	Calcite	Aragonite	Muscovite Illite	Kaolinite	Microcline	Hematite	Pyrite	Amorphous Phase
Escucha sandstone Mave site	94.8	0	0.4	0.4	0.3	3.4	0.3	0.2	0.2
Utrillas sandstone Devesa site	94.3	0.7	0	0.9	0.2	3.7	0.1	0	0.1
Utrillas sandstone Olleros site	94.1	0.4	0.1	0.9	0.2	3.9	0.2	0.1	0.1

4.3. Petrophysical Characterization

The obtained hydraulic properties confirmed the differences in the pore space structure of the Utrillas and Escucha sandstones (Table 4). The results provided by different methods are in good agreement, indicating significantly higher porosity, water uptake and permeability values in the Escucha sandstones than in the Utrillas sandstones.

Table 4. Mean values of hydraulic properties carried out by different techniques for Escucha and Utrillas sandstones.

Samples	AUTOSORC			Le Chatelier Pycnometer					Gas Permeameter
	Bulk Density (Kg/m^3)	Open Porosity (%)	Saturated Water Content (%)	Density (Kg/m^3)		Porosity (%)			$K_{Klinkenberg}$ (mD)
				Bulk	Skeletal	Open	Closed	Total	
Escucha sandstone Mave site	2006	24.18	12.05	2017	2668	23.11	1.30	24.41	90
Utrillas sandstone Devesa site	2310	14.45	6.20	2336	2687	12.69	0.38	13.07	30
Utrillas sandstone Olleros site	2302	13.87	6.09	2440	2692	12.63	0.42	13.05	40

According to the MICP analysis, the pore space of the Escucha sandstones is characterized by a large number of macropores, which are connected by abundant channels of large radii (15.92 μm), forming a well-communicated pore network of low tortuosity (Table 5 and Figure 7). Its open porosity according to this method is about 26%. On the other hand, in the Utrillas sandstone, the micropores are dominant (Figure 7). The pore network is also well connected but the pore throats are of smaller

radii (0.26 µm–Devesa site; 7.00 µm-Olleros site), and the tortuosity of the system is somewhat higher (Table 5). These characteristics can be generalized for the whole Utrillas sandstone despite of the important heterogeneity observed between the two study areas, as well as within the samples of the same zone, as demonstrated by the mercury intrusion curves of Figure 7.

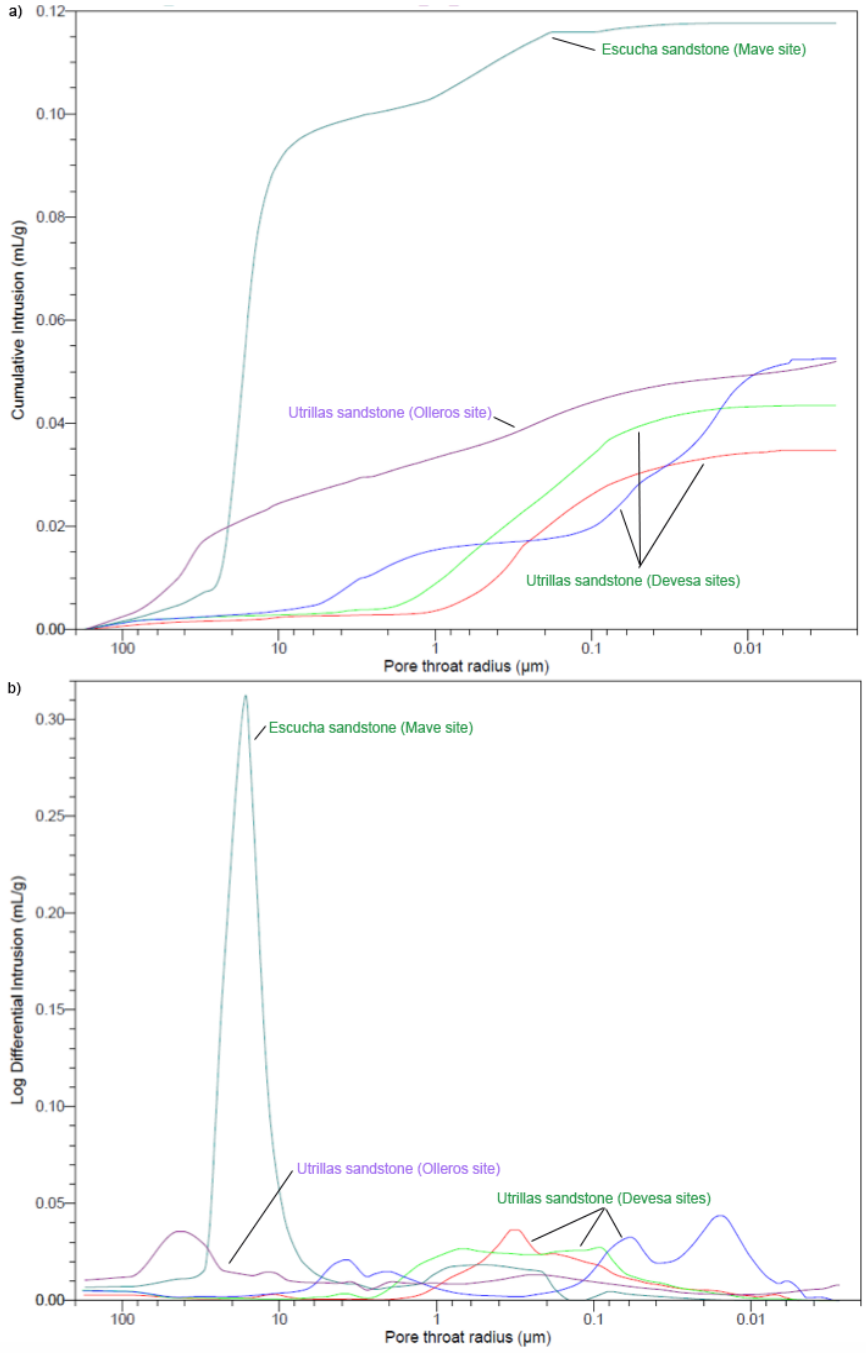

Figure 7. Typified mercury intrusion curves (**a**) and pore throat radius distribution (**b**) of the studied sandstones. The homogeneous Escucha sandstones can be represented by a single typified curve (dark green), while for the Utrillas sandstones four typified curves were obtained: one for the Olleros site (purple) and three for the Devesa site (red, blue and light green).

The 3D modelling of the pore space allowed us to visualize the configuration of channels and pores (both open and trapped) in a simplified manner, and to simulate fluid flow through them

(Figure 8). The modelling results verify the characteristics described before, as they highlight the well-connected porosity of low tortuosity in both sandstones with a higher porosity value and pore sizes in case of the Escucha sandstones. In the Escucha sandstone, another interesting feature was also captured by the model, namely the presence of mm scale layers of lower porosity that correspond to beds of finer grain size, which is in accordance with the outcome of the ultrasound measurements. These layers are responsible for the fact that the average water permeability value calculated by the software is lower for the Escucha formation than for the Utrillas formation.

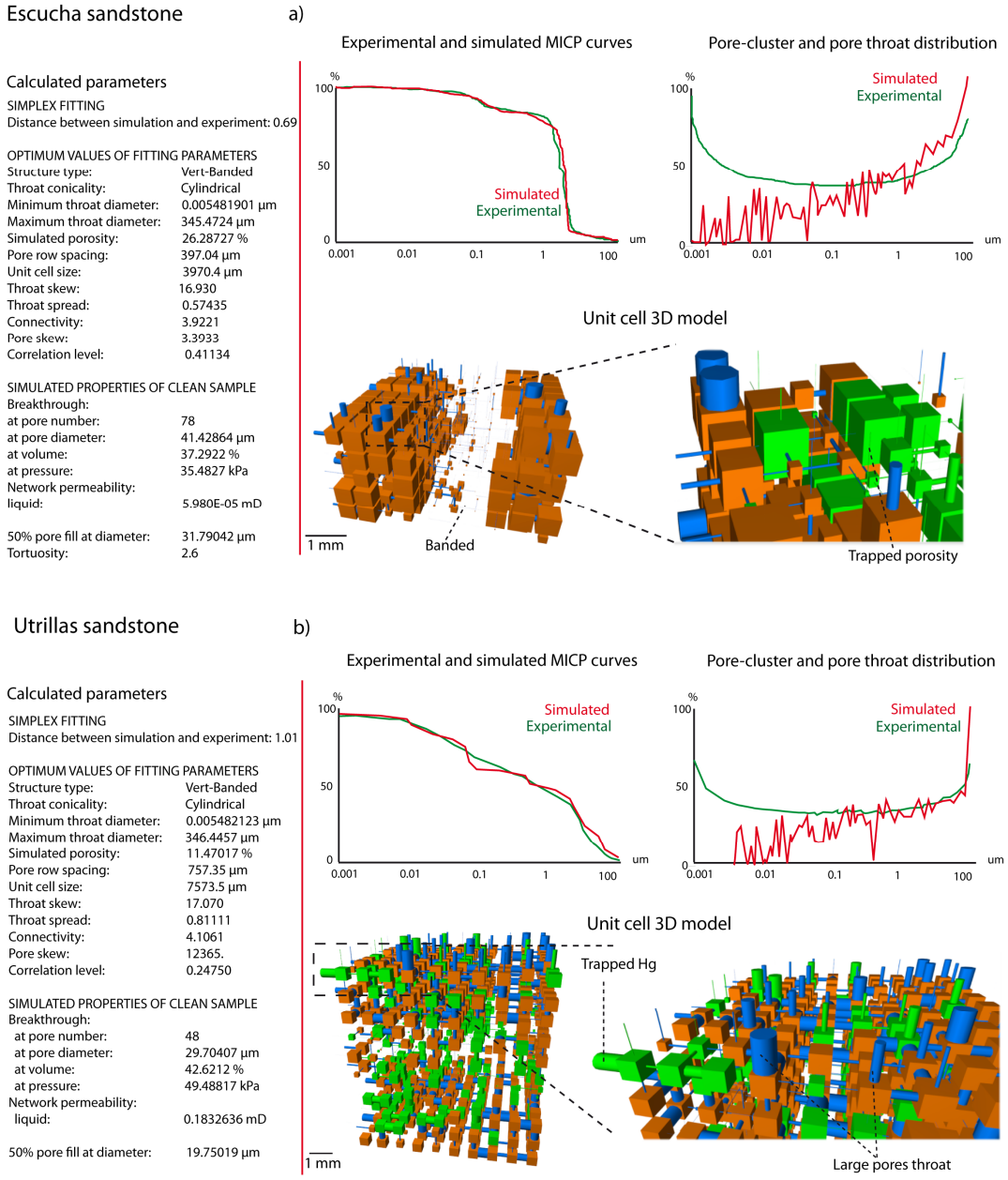

Figure 8. Example of pore space modelling by the Pore-Cor software in the Escucha formation (**a**) and the Utrillas formation (**b**). The software creates a simulated intrusion curve based on the experimental one and uses it as the basis of the 3D modelling. Information about pore and pore throat size distribution, calculated parameters and the unit cell are also displayed. In the visual representation of the unit cell of the 3D model, pores are depicted as cubes, channels as cylinders and different colors show the open and trapped porosity. The "Network permeability" value calculated by the software is a liquid percolation value.

Table 5. Porosimetric parameters obtained by means of MICP.

Samples		Bulk Density (Kg/m^3)	Skeletal Density (Kg/m^3)	Open Porosity (%)	Pore Throat Radius (μm)		Characteristic Length (μm)	Specific Surface (m^2/g)	Connectivity	Tortuosity
					Average	Median				
Escucha sandstone (Mave sites)		1856	2693	26.25	1.54	15.92	17.51	0.15	4.63	5.76
Utrillas sandstone	Devesa site	2382	2689	10.275	0.08	0.21	5.46	1.71	2.45	59.65
	Olleros site	2413	2689	12.27	0.06	7.00	47.42	1.65	3.06	12.96

5. Discussion

According to [1,4,13], in a preliminary phase of site characterization for CO_2 geological storage the following aspects should be taken into consideration: (i) an adequate storage capacity and injectivity; (ii) a satisfactory sealing caprock or confining unit and (iii) a sufficiently stable geological environment (integrity of the storage site). The overall assessment of these criteria is beyond the scope of this paper, as this study is only concerned with a rock matrix scale petrographic and petrophysical characterization of the selected reservoir formations, in order to provide a basis for further research. The study of the target Utrillas and Escucha sandstones by means of OpM, SEM, OIA, XRD and XRF allowed us to thoroughly assess their petrographic characteristics. On the other hand, the applied petrophysical measurements yielded detailed information about the pore space configuration and the facility of fluid flow through the studied rocks [35,36]. This data provides fundamental input for further storage capacity and injectivity assessment at rock matrix scale.

The obtained results showed that both sandstone varieties (Escucha and Utrillas) are characterized by 95% quartz content and heterogeneous rock texture with a widely varying range of petrophysical parameters.

The petrographic and chemical characterization of the rocks makes it possible to assess likely chemical reactions in a CO_2-brine-rock system. The reactivity of sandstones under CO_2 storage conditions has been extensively studied in the literature revealing the importance of these [37]. According to [37,38], mineral dissolution has been found to affect not only the carbonate components but also other rock forming minerals typically present in sandstones (i.e., plagioclase, biotite, clay minerals, etc.). Besides, in some experiments, precipitation of new mineral phases (carbonates) has also been observed. According to References [8,39–41], the precipitation and dissolution of minerals could produce increasing or decreasing permeability and porosity, loss of injectability and strength reduction or strength gain. In our case, SiO_2 dominate the rock composition, which is favorable, as far as reactivity is concerned. Under the conditions of CO_2 geological storage in these rocks, potassium feldspar and mica dissolution would be the principal potentially occurring processes [37,38]. Nevertheless, the resulting effects of these reactions could be further studied by means of laboratory experiments and geochemical modelling. Given the dominantly silicate composition of the reservoir rock, the expected trapping mechanisms are structural/stratigraphic trapping, residual trapping and solubility trapping [14].

The exhaustive characterization of the rock types by measurement of ultrasound propagation and hydraulic properties, together with the simplified modelling of their porous network, revealed the important differences in their hydraulic functionality considering both storage capacity and fluid flow (i.e., injectivity). The highly heterogeneous nature of the Utrillas sandstones, caused by variability in the rock texture (i.e., layers of finer and coarser grain size) was also demonstrated. This heterogeneity requires further comprehensive sampling and characterization campaigns of the target storage formations based on in-situ measurements and deep borehole sampling for the proper assessment of the overall petrophysical characterization of potential reservoir structures.

Porosity parameters were calculated based on the data of several methods and techniques (OIA, MICP, GPT, HT) of different scales (both 2D and 3D) (Tables 1, 4 and 5). The obtained results are in

good agreement with each other, and they confirmed the heterogeneous nature of the materials, as the porosity values range between 8–26%. Comparing the three studied varieties, the Escucha sandstones have more favorable characteristics than both Utrillas varieties concerning all of the relevant parameters (open porosity, permeability, connectivity, etc.). Nonetheless, according to research data from CO_2 storage studies in saline aquifers from all over the world [13] (Table 6), these values fall within the cautionary to positive indicators range considering storage site suitability. The measured values, however, are only representative of the studied rock matrix scale and do not provide information about porosity composed of macro-fractures on the rock massif scale. On the other hand, the obtained permeability values were found to be far below the recommended ranges, at least on the studied rock matrix scale. This outcome calls for further permeability studies both by the application of more specific laboratory scale techniques (i.e., liquid and relative permeability measurements) and by targeted in-situ, field-scale injectivity and permeability testing.

Table 6. Key geological indicators for storage site suitability [13] and their assessment for the studied rock types and potential reservoir structures (Figure 1a).

Reservoir Properties	Positive Indicators (PI)	Cautionary Indicators (CI)	Escucha Mave Site	Utrillas Devesa Site	Utrillas Olleros Site
Depth	>1000 m <2500 m	>800 m <2500 m	PI	PI	PI
Reservoir thickness	>50 m	>20 m	PI	PI	PI
Porosity	>20%	<10%	PI	PI	PI
Permeability	>500 mD	<200 mD	CI	CI	CI
Stratigraphy	Uniform	Complex lateral variation and complex connectivity of reservoir facies	PI	PI	PI

Finally, the applied methodology proved the applicability of MICP 3D modelling based on a simulated mercury intrusion curve, at least in the case of materials with high open porosity, well-connected pore network and Gaussian-type pore throat size distribution. The parameters obtained by the simulation are in good agreement with the results obtained by direct measurements concerning porosity and hydraulic functionality. The large discrepancy between the experimental gas permeability and the simulated liquid permeability values requires further verification of the model, however. Overall, this method can offer a fast, simple and relatively economic tool for preliminary studies of CO_2 reservoir formations sampled in surface outcrops. Possible differences between outcrop samples and the reservoir at depth must be taken into consideration. According to [10], at the rock matrix scale there is a predictable reduction in the pore structure with depth owing to the effects of compaction and/or cementation, primarily as quartz overgrowths. Nevertheless, at the rock massif scale, the porosity is expected to increase due to the presence of large scale fractures.

6. Conclusions

Qualitative and quantitative assessments of petrography and mineralogy by OpM, SEM and OIA can be important tools for geosciences, providing numerical values for the interpretation of the rock texture and mineralogy. Furthermore, petrophysical studies offer useful information in the assessment of how pores are interconnected at the rock matrix scale. For this study, the Escucha and Utrillas sandstones were selected due to their potential as CO_2 reservoir in Spain. However, the same methodology could be applicable for other studies related to CO_2 reservoirs.

The petrographic and petrophysical characterization of the materials sampled in surface outcrops at the Mave, Devesa and Olleros sites provided a large amount of valuable information about the studied levels of detrital reservoir rocks contributing significantly to the assessment of the potential of these rock formations for CO_2 storage in deep saline aquifers. This approach therefore, could offer a powerful tool in the initial screening phases of site selection for industrial scale CO_2 storage projects.

The petrophysical characterization carried out at the rock matrix scale (Tables 4 and 5) indicates that the studied sandstones, and especially the Escucha sandstones, have a considerable open porosity and a large number of pores, which is a favorable factor for storage capacity. Abundant channels

of large radii connect the pores forming a relatively well-communicated network of low tortuosity, which suggests medium to high hydraulic connectivity at the rock matrix scale. However, the measured air permeability could be considered medium-low for this rock type, and certain deviation of data obtained by other methods (i.e., MICP and 3D modelling) was found. The observed heterogeneity, the low permeability values and the limited scale of the study (i.e., rock matrix scale) highlight the importance of in-situ, field-scale characterization campaigns and reservoir-scale modelling for the overall assessment of the suitability of the studied formations for CO_2 storage.

Author Contributions: Conceptualization, F.M. and T.K.; Methodology, E.B.; Software, E.B.; Validation, F.M., T.K. and E.B.; Formal Analysis, T.K.; Investigation, E.B.; Resources, E.B.; Data Curation, F.M.; Writing-Original Draft Preparation, E.B.; Writing-Review & Editing, T.K.; Visualization, F.M.; Supervision, E.B.; Project Administration, E.B.; Funding Acquisition, E.B.

Funding: This research was funded by [ALGECO2-IRMC Project] grant number [2294-2013] and [CO_2-Pore Project] grant number [2009-10934, FEDER-UE].

Acknowledgments: The authors would like to thank the funding provided through the ALGECO2-IRMC Project (Instituto Geológico y Minero de España: 2294-2013), CO2-Pore Project (Plan Nacional de España: 2009-10934, FEDER-UE). Thanks are due to Luis Quintana (IGME) for providing help in geological setting description.

Conflicts of Interest: The authors declare no conflict of interest.

Abbreviations

The following abbreviations are used in this manuscript:

OpM	Optical Microscopy
SEM	Scanning Electron Microscopy
OIA	Optical Image Analysis
XRF	X-ray fluorescence
XRD	X-ray diffraction
MICP	Mercury injection capillary pressure
GPT	Gas permeameter test
HT	Hydraulic test
CCS	Carbon Capture and Storage
DB	Duero basin
NDT	Non-destuctive technique
Vp	P-wave velocity
Ro	Roundness
As	Aspect
D	Dimensions
PI	Positive indicators
CI	Cautionary indicators

References

1. Bachu, S. Sequestration of CO_2 in geological media: Criteria and approach for site selection in response to climate change. *Energy Convers. Manag.* **2000**, *41*, 953–970. [CrossRef]
2. Gaus, I. Role and impact of CO_2-rock interactions during CO_2 storage in sedimentary rocks. *Int. J. Greenh. Gas Control* **2010**, *4*, 73–89. [CrossRef]
3. Garía-Lobón, J.L.; Reguera-García, M.I.; Martín-León, J.; Rey-Moral, C.; Berrezueta, E. *Plan de Selección y Caracterización de Áreas y Estructuras Favorables para el Almacenamiento Geológico de CO2 en España. Resumen Ejecutivo*; Instituto Geológico y Minero de España (IGME): Madrid, Spain, 2010.
4. Bacci, G.; Korr, A.; Durucan, S. Experimental investigation into salt precipitation during CO_2 injection in saline aquifers. *Energy Procedia* **2011**, *4*, 4450–4456. [CrossRef]
5. Benson, S.B.; Cole, D.R. CO_2 sequestration in deep sedimentary formations. *Elements* **2008**, *4*, 325–331. [CrossRef]

6. Izeg, O.; Demiral, B.; Bertin, H.; Akin, S. CO_2 injection into saline carbonate aquifer formations I: Laboratory investigation. *Transp. Porous Media* **2008**, *72*, 1–24.
7. Berrezueta, E.; Ordóñez-Casado, B.; Quintana, L. Qualitative and quantitative changes in Detrital reservoir rocks caused CO_2-brine-rock interactions during first injection phases (Utrillas sandstones, Northern Spain). *Solid Earth* **2016**, *7*, 37–53. [CrossRef]
8. Campos, R.; Barrios, I.; Lillo, J. Experimental CO_2 injection: Study of phisycal changes in sandstone porous media using HG Porosimetry and 3D pore network models. *Energy Rep.* **2015**, *1*, 71–79. [CrossRef]
9. Llamas, B.; Álvarez, R.; Mazadiego, L.F.; Loredo, J.; Cámara, A. Estudio de afloramientos de unidades detríticas como posibles almacenes geológicos de CO_2 en la Cuenca del Duero (España). *Estudios Geológicos* **2014**, *70*, e008. [CrossRef]
10. Medina, C.; Rupp, J.; Barnes, D. Effects of reduction in porosity and permeability with depth on storage capacity and injectivity in deep saline aquifers: A case study from the Mount Simon Sandstone aquifer. *Int. J. Greenh. Gas. Control* **2011**, *17*, 411–422. [CrossRef]
11. Suarez-González, A.; Kovács, T.; Herrero-Hernández, F.; Gómez-Fernandez, F. Petrophysical characterization of the Dolomitic member of the Boñar Formation (Upper Cretaceous; Duero basin, Spain) as a potential CO_2 reservoir. *Estudios Geológicos* **2016**, *72*, e048.
12. Saeedi, A.; Rezaee, R.; Evans, B.; Clennell, B. Multiphase flow behaviour during CO_2 geo-sequestration: Emphasis on the effect of cyclic CO_2-brine flooding. *J. Pet. Sci. Eng.* **2011**, *79*, 65–85. [CrossRef]
13. Chadwick, A.; Arts, R.; Bernstone, C.; May, F.; Thibeau, S.; Zweigel, P. *Best Practice for the Storage of CO_2 in Saline Aquifers. Observations and Guidelines form SACS and CO_2STORE Projects*; British Geological Survey (BGS): Keyworth, Notthingam, UK, 2008.
14. Intergovernmental Panel on Climate Change. *Special Report on Carbon Dioxide Capture and Storage*; Metz, B., Davidson, O., de Coninck, H., Loos, M., Meyer, L., Eds.; Cambridge University Press: Cambridge, UK; New York, NY, USA, 2005; p. 442.
15. Martínez, R.; Suárez, I.; Carneiro, J.; Zarhloule, Y.; Le Nindre, Y.; Boavida, D. Storage capacity evaluation for development of CO_2 infrastructure in the west Mediterranean. *Energy Procedia* **2013**, *37*, 5209–5219. [CrossRef]
16. Arenillas, A.; Mediato, J.; García, J.; Molinero, R.; Catalina, R. *Atlas de Estructuras del Subsuelo Susceptibles de Almacenamiento Geológico de CO2 en España*; Suarez-Díaz, I., Ed.; Instituto Geológico y Minero de España: Madrid, Spain, 2014; p. 211.
17. Gallastegui, J. Estructura cortical de la cordillera y margen continental cantábricos: Perfiles ESCI-N. *Trabajos de Geología* **2000**, *22*, 9–231.
18. Arnáiz, I.; Robles, S.; Pujalte, V. Correlación entre registros de sondeos y series de superficie del Aptiense-Albiense continental del extremo SW de la Cuenca Vascocantábrica y su aplicación a la identificación de zonas lignitíferas. *Geogaceta* **1991**, *10*, 65–68.
19. Alonso, J.L.; Pulgar, J.A.; García-Ramos, J.C.; Barba, P. Tertiary basins and Alpine tectonics in the Cantabrian Mountains (NW Spain). In *Tertiary Basins of Spain: The Stratigraphic Record of Crustal Kinematics*; Friend, P.F., Dabrio, C.J., Eds.; Cambridge University Press: Cambridge, UK, 1996; pp. 214–227.
20. López Olmedo, F.; Enrile Alvir, A.; Cabra Gil, P. *Mapa Geológico de España. 1: 50.000. Hoja num. 133 (Prádanos de Ojeda) Segunda Serie MAGNA, Primera Edición*; Instituto Geológico y Minero de España (IGME): Madrid, Spain, 1997.
21. Espina, R.G. La Estructura y Evolución Tectonoestratigráfica del Borde Occidental de la Cuenca Vasco Cantábrica (Cordillera Cantábrica, NO de España). Ph.D. Thesis, University Oviedo, Oviedo, Spain, 1996.
22. Ambrose, T.; Carballeira, J.; López-Rico, J.; Wagner, R.H. *Mapa Geológico de España. 1: 50:000, Hoja núm. 107 (Baruelo de Santullan)*; Segunda Serie MAGNA; Instituto Geológico y Minero de España (IGME): Madrid, Spain, 1978.
23. Aróstegui, J.; Irabien, M.J.; Sangüesa, J.; Zuluaga, M. La Formación de Utrillas en el borde sur de la cuenca Vasco-Cantábrica: Aspectos estratigráficos, mineralógicos y genéticos. *Estudios Geológicos* **2000**, *56*, 251–267. [CrossRef]
24. Montoto, M. *Petrophysics at the Rock Matrix Scale: Hydraulic Properties and Petrographic Interpretation*; Publicación técnica 11/2003; ENRESA: Madrid, Spain, 2003; p. 297.
25. Mateos, F. Caracterización Pertrofísica del Acuífero Costero de Campos (Mallorca). Funcionalidad Hidráulica de su Porosidad. Ph.D. Thesis, Universidad de Oviedo, Oviedo, Spain, 2011.

26. Alonso, F.J.; Esbert, R.M.; Ordaz, J. Comportamiento hídrico de calizas y dolomías. *Boletín Geológico y Minero* **1987**, *94*, 108–130.
27. Hilpert, M.; Miller, C.T. Pore morphology simulation of drainage in totally wetting porous media. *Adv. Water Resour.* **2001**, *24*, 243–255. [CrossRef]
28. Mosquera, M.J.; Rivas, T.; Prieto, B.; Silva, B. Capillary rise in granitics rock: Interpretation of kinetics on the basis of pore structure. *J. Colloid Interface Sci.* **2000**, *222*, 41–45. [CrossRef] [PubMed]
29. Tournier, B.; Jeannette, D.; Destrigneville, C. Stone drying: An approach of the effective evaporating surface area. In Proceedings of the 9th International Congress on Deterioration and Conservation of Stone, Venice, Italy, 19–24 June 2000; pp. 625–635.
30. Tsakiroglou, C.D.; Payatakes, A.C. Characterization of the pore structure of reservoir rocks with the aid of serial sectioning analysis, mercury porosimetry and network simulation. *Adv. Water Resour.* **2000**, *23*, 773–789. [CrossRef]
31. Del Ferro, N.; Berti, A.; Francioso, O.; Ferrari, E.; Matthews, G.P.; Morari, F. Investigating the effects of wettability and pore size distribution on aggregate stability: The role of soil organic matter and the humic fraction. *Eur. J. Soil Sci.* **2012**, *63*, 152–164. [CrossRef]
32. Levi, C.L.; Matthews, G.P.; Laudone, G.M.; Gribble, C.M.; Turner, A.; Ridway, C.J.; Gerard, D.E.; Schoelkopf, J.; Gane, P.A.C. Diffusion and Tortuosity in Porous Functionalized Calcium Carbonate. *Ind. Eng. Chem. Res.* **2015**, *54*, 9938–9947. [CrossRef]
33. Berrezueta, E.; González-Menéndez, L.; Ordóñez-Casado, B.; Olaya, P. Pore network quantification of sandstones under experimental CO_2 injection using image analysis. *Comput. Geosci.* **2015**, *77*, 97–110. [CrossRef]
34. Buij, O.; Gisbertt, J. Quantification of the porosity on sandstones in digital image analysis. *Geogaceta* **2007**, *41*, 35–38.
35. Wu, H.; Zhang, C.; Ji, Y.; Liu, R.; Wu, H.; Zhang, Y.; Geng, Z.; Zhang, Y.; Yang, J. An improved method of characterizing the pore structure in tight oil reservoirs: Integrated NMR and constant-rate-controlled porosimetry data. *J. Pet. Sci. Eng.* **2018**, *166*, 778–796. [CrossRef]
36. Veloso, F.; Frykman, P.; Nielsen, C.M.; Soria, A.R.; Meléndez-Hevia, N. Outcrop scale reservoir characterisation and flow modelling of CO_2 injection in the tsunami and the barrier island-tidal inlet reservoirs of the Camarillas Fm. (Galve Sub-basin, Teruel, NE Spain). *Int. J. Greenh. Gas Control* **2016**, *55*, 60–72. [CrossRef]
37. Kaszuba, J.P.; Janecky, D.R.; Snow, M.G. Carbon dioxide reaction processes in a model brine aquifer at 200 °C and 200 bars: Implications for geologic sequestration of carbon. *Appl. Geochem.* **2003**, *18*, 1065–1080. [CrossRef]
38. Fischer, S.; Liebscher, A.; De Lucia, M.; Hecht, L. Reactivity of sandstone and siltstone samples from the Ketzin pilot CO_2 storage site-Laboratory experiments and reactive geochemical modelling. *Environ. Earth Sci.* **2013**, *70*, 3687–3708. [CrossRef]
39. Berrezueta, E.; Kovacs, T. Application of optical image analysis to the assessment of pore space evolution after CO_2 injection in sandstones. A case study. *J. Pet. Sci. Eng.* **2017**, *159*, 679–690. [CrossRef]
40. Edlman, K.; Niemi, A.; Bensabat, J.; Haszeldine, R.S.; McDermott, C.I. Mineralogical properties of the caprock and reservoir sandstone of the Heletz field scale experimental CO_2 injection site, Israel; and their initial sensitivity to CO_2 injection. *Int. J. Greenh. Gas. Control* **2016**, *48*, 94–104. [CrossRef]
41. Kharaka, Y.K.; Cole, D.R.; Hovorka, S.D.; Gunter, W.D.; Knauss, K.G.; Freifeld, B.M. Gas–water–rock interactions in Frio formation following CO_2 injection: Implications for the storage of greenhouse gases in sedimentary basins. *Geology* **2006**, *34–37*, 577–580. [CrossRef]